FPGA based Fuzzy Logic Controller for Frequency Regulation of Synchronous Generator

Rajiv Bishwokarma
Kathmandu University
Dhulikhel, Nepal
rajivbishwokarma@outlook.com

Shayarrn Khatiwoda
Kathmandu University
Dhulikhel, Nepal
shayarrn@gmail.com

Bishal Bhetwal
Kathmandu University
Dhulikhel, Nepal
bishalbhetwal@outlook.com

Shailendra Kumar Jha
Kathmandu University
Dhulikhel, Nepal
shailendra@ku.edu.np

***Abstract*— This paper details the design and implementation of a type-I fuzzy logic controller for the regulation of the frequency of a synchronous generator under varying load conditions in the laboratory setup. The fuzzy system thus developed is integrated into the FPGA platform with the intention of making an assessment of the performance of the system in the real power system. An expert reference is taken to design the fuzzy logic set for input and output linguistic variables. At the initial stage of the crisp value of the frequency of the synchronous generator under the consideration is given to the fuzzification unit of the controller. The fuzzified input is then evaluated based on the predefined rule base which leads to the calculation of the fuzzified output. The fuzzified output is then de-fuzzified to finally generate the required pulse width modulated duty cycle; it is then fed into the MOSFET based chopper controller to appropriately regulate the input voltage of the prime mover that drives the synchronous generator. In the final stage, the controller is developed into an FPGA unit and then experimented with, at the laboratory to develop an understanding of the reliability and stability of the generated output PWM.**

Keywords—Fuzzy Logic, Fuzzy Controller, Synchronous Generator, Frequency Control, Field Programmable Gate Array

I. INTRODUCTION

The control of the frequency parameter of the synchronous generator is a topic of interest for researchers cumulating numerous researches in literature with different controller schemes [6-11]. Power system implemented synchronous generator experiences fluctuations and disturbances that are random and thus unpredictable and non-linear [1] but the controlling of the randomly varying frequency of generated power in power system, within predefined limits of fluctuation is vital for the excellent quality of power production [2]. Using controllers with feedback to the power system with aim of correcting any aberrant changes in the frequency parameter is used to control the frequency within tolerable limits, as control of frequency with feedback reduces power system oscillations and thus contributes to reduced wear on the synchronous generator's rotor and other mechanically coupled rotating parts which manifest into more reliable transient stability [3]. Digital systems with their ever-increasing speed of operation outpperform human operators in comparison considering quickness and accuracy of response and fuzzy logic-based system have gained popularity among systems that takes input change that is not gradual but abrupt

[4]. Fuzzy logic controllers can be optimized for application-specific control systems by capitalizing on expert's input that can replicate control methods and techniques of a human controller but with a higher degree of resilience and speed [5].

Field programmable gate array (FPGA) is an integrated circuit that can be programmed and modified in the field after manufacture. FPGA has three basic building blocks namely logic gates, flip-flops and memories, and wires [12]. The FPGA-based system offers the ability to reprogram the system, be it to fix bugs, modify control logic or update system performance making it ideal for control implementation of the system as dynamic as a power system that has the characteristics of continual improvement or modification over its lifetime [13]. Microcontrollers are a viable option only if the computational needs are small but, for greater computational needs, digital signal processors are best suited [14]. Furthermore, poor performance is commonplace on DSP systems, if implemented in inherently sequential processing hardware, requiring extremely efficient scheduling of algorithmic process demanding the use of parallel processing architecture [15]. FPGAs have advantages of increased bandwidth with multiple multipliers and accumulate cells on a single chip, over programmable digital signal processors [16].

In our experimental setup in the laboratory, we have designed the frequency of the synchronous generator to be the function of the DC motor's speed. The DC motor is mechanically coupled to the rotor of the synchronous generator. The shaft speed of the rotor can be controlled through the governor system developed as described in this paper; in real power system; so can the frequency of the power by monitoring the shaft speed of the generator.

The objective of this paper is to develop fuzzy-rules based on the aforementioned relationship and extract expert data based on experiments to create an FPGA based fuzzy controller for frequency control of a synchronous generator. The FPGA-based system offers the ability to reprogram the system making it ideal for control implementation of the system as dynamic as a power system that has the characteristics of continual improvement or modification over its lifetime.

II. SYSTEM MODEL

Let us consider an arbitrary power system that receives its power from a synchronous generator. Considering that this power line bus is not infinite, we can assume that the change in load causes disturbances in the frequency of the power system. Our objective is to control this frequency and regulate it between the desired thresholds.

978-1-7281-5846-4/20/$31.00 ©2020 IEEE

A real power system makes use of a governor mechanism to control and regulate the frequency of the power system by compensating for required power input with more inflow of fuel and in attempt to mimic that phenomena in lab we have coupled a DC motor to the rotor's shaft of the synchronous generator and control of the rotor speed ensures regulation of frequency of power system. The block diagram for the system is shown in Fig 1.

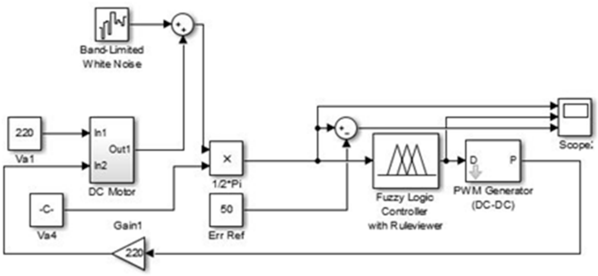

Fig. 1. Simulink model of the system

Consider a separately excited DC motor. The instantaneous field current,

$$i_f = \frac{Vf}{Rf+sLf} \tag{1}$$

Where V_f is the excitation or field voltage, L_f, field inductance and, R_f, *the* resistance of the field.

The instantaneous field current,

$$i_a = \frac{V-Eg}{Ra+sLa} \tag{2}$$

Where V_a is the output or armature voltage, R_a is armature resistance, L_a is armature inductance, E_g is induced back emf. The output V_a is controlled with the PWM generator that is controlled with the duty cycle generated from the fuzzy controller as per the developed algorithm which maps the frequency of the system to a particular duty cycle.

The motor back emf and torque developed given by

$$Eg = K_v \omega_m i_f \tag{3}$$

$$\mathrm{T}d = K_t \omega_m i_f \tag{4}$$

The load torque must be equal to the developed torque.

$$\mathrm{T}l = Js\omega m + B\omega m \tag{5}$$

The speed of the motor is given by the equation:

$$Wm = \frac{Va - IaRa}{KvIf} \tag{6}$$

Where, K_v: voltage constant, ω_m: motor speed, K_t: torque constant, J_s: coefficient for the moment of inertia, and B: coefficient of viscous friction.

From equation (1), (3), (4) and (5) we can obtain the transfer function of DC Motor as:

$$\frac{Wm(s)}{Ea(s)} = H(s) = \frac{Kt}{(Ra + sLa)(B + sJ) + KtKv} \tag{7}$$

Assuming that the system operates at steady state with speed error (Werr) maintained in margin ±10 Hz, the characteristic curve (Fig. 4) of the implemented fuzzy system can be approximated by a straight line as:

$$1 - r(t) \tag{8}$$

In its range 40Hz to 60Hz, where is r(t) is ramp function.

Table 2 gives us the maximum and minimum value Fuzzy Logic Controller takes. Normalizing (8) in for given value we get,

$$0.96 - 0.92r(t) \tag{9}$$

The transfer function of the FIS at steady state is:

$$\frac{Ea(s)}{Werr(s)} = G(s) = Vp(\frac{0.96s - 0.92}{s^2}) \tag{10}$$

The closed-loop steady-state transfer function for the negative feedback loop will be given as:

$$\frac{C(s)}{R(s)} = Q(s) = \frac{G(s)}{1 + G(s)H(s)} \tag{11}$$

In our model, we implement armature voltage control of the DC motor. The DC motor reaches its maximum speed of 300rpm corresponding to the frequency of 50Hz as required by our system at a 0.5 duty cycle. The 0.5 duty cycle corresponds to approximately half of the rated voltage of the used DC motor and allows the controlled armature voltage to swing from 0V to 220V giving equal control range on both sides without exceeding the rated voltage limit of the DC motor. This optimization is attainted by controlling the field excitation of the DC motor to a constant value which allows for 3000rpm speed at 110V in armature windings. For the simulation results to be an accurate representation of the real power system the noise input in the simulation has been modeled to be equivalent to the disturbance that is moderate to severe and is laboratory representative of abrupt load changes in the power system. The fuzzy controller is highly sensitive to larger deviation and gradually less sensitive to smaller deviation from nominal frequency which translates to the fact that it tries to bring the system to equilibrium quickly if the frequency deviation is too large and slowly and carefully with more sampling instances closer to the nominal frequency. The controller is modeled to be insensitive in the region adjacent to the nominal value of 50Hz on both sides from 48Hz to 52Hz to reduces oscillation in this region as high-frequency oscillation contributes to reduced quality of power. The system behavior can be observed in Fig. 4. All membership function span 4Hz range composed of triangular membership functions except central and outermost ones which are trapezoidal as described above and shown in Fig. 2. Their mathematical description is given in equations (12) to (20):

$$-E = \left\{ \begin{array}{c} 1, if\ 0 \le f\ \le 40 \\ \frac{40 - x}{2}, if\ 0 \le f\ \le 40 \\ 0, if\ f > 42 \end{array} \right\} \tag{12}$$

$$-L = \left\{ \begin{array}{c} 0, if\ f < 40 \\ \frac{x - 40}{2}, if\ 40 \le f\ \le 42 \\ \frac{42 - x}{2}, if\ 42 \le f\ \le 44 \\ 0, if\ f > 44 \end{array} \right\} \tag{13}$$

$$-M = \left\{ \begin{array}{c} 0, if\ f < 42 \\ \frac{x - 42}{2}, if\ 42 \le f\ \le 44 \\ \frac{46 - x}{2}, if\ 44 \le f\ \le 46 \\ 0, if\ f > 46 \end{array} \right\} \tag{14}$$

$$-S = \left\{ \begin{array}{c} 0, if\ f < 44 \\ \frac{x - 44}{2}, if\ 44 \le f\ \le 46 \\ \frac{48 - x}{2}, if\ 46 \le f\ \le 48 \\ 0, if\ f > 48 \end{array} \right\} \tag{15}$$

978-1-7281-5846-4/20/$31.00 ©2020 IEEE

$$N = \begin{Bmatrix} 0, if\ f < 46 \\ \frac{x-46}{2}, if\ 46 \le f\ \le 48 \\ 1, if\ 48 \le f\ \le 52 \\ \frac{52-x}{2}, if\ 50 \le f\ \le 52 \\ 0, if\ f > 52 \end{Bmatrix} \quad (16)$$

$$+S = \begin{Bmatrix} 0, if\ f < 50 \\ \frac{x-50}{2}, if\ 50 \le f\ \le 52 \\ \frac{54-x}{2}, if\ 52 \le f\ \le 54 \\ 0, if\ f > 54 \end{Bmatrix} \quad (17)$$

$$+M = \begin{Bmatrix} 0, if\ f < 52 \\ \frac{x-52}{2}, if\ 52 \le f\ \le 54 \\ \frac{56-x}{2}, if\ 54 \le f\ \le 56 \\ 0, if\ f > 56 \end{Bmatrix} \quad (18)$$

$$+L = \begin{Bmatrix} 0, if\ f < 54 \\ \frac{x-54}{2}, if\ 54 \le f\ \le 56 \\ \frac{58-x}{2}, if\ 56 \le f\ \le 58 \\ 0, if\ f > 58 \end{Bmatrix} \quad (19)$$

$$+E = \begin{Bmatrix} 0, if\ 0 \le f\ \le 58 \\ \frac{x-58}{2}, if\ 58 \le f\ \le 60 \\ 1, if\ f > 60 \end{Bmatrix} \quad (20)$$

The fuzzy controller's output membership functions span from the duty cycle of 0 to 1 with a nominal value of frequency for the unloaded power system corresponding to the duty cycle of 0.5 as describe previously.

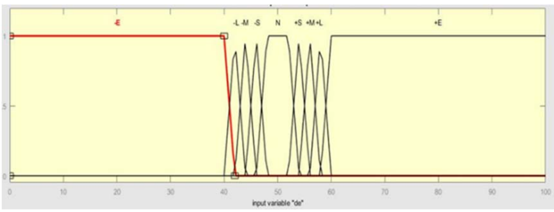

Fig. 2. Input membership functions

The rotor speed is 3000rpm at this duty cycle and the corresponding armature voltage is 110V. As the loading of the system changes dynamically, the duty cycle also changes with respect to the change in load as per the algorithm of the controller. The intermediate membership function for output or the duty cycle is triangular except for ones at the ends which are trapezoidal as shown in Fig. 3. The span of each intermediate duty cycle membership function is 0.125 and their mathematical description follows.

$$a = \begin{Bmatrix} 1, if\ DC < 0 \\ \frac{0.125-x}{0.125}, if\ 0 \le DC\ \le 0.125 \\ 0, if\ DC > 0.125 \end{Bmatrix} \quad (21)$$

$$b = \begin{Bmatrix} 0, if\ DC < 0 \\ \frac{x-0}{0.125}, if\ 0 \le DC\ \le 0.125 \\ \frac{0.25-x}{0.125}, if\ 0.125 \le DC\ \le 0.25 \\ 0, if\ DC > 0.25 \end{Bmatrix} \quad (22)$$

$$c = \begin{Bmatrix} 0, if\ DC < 0.125 \\ \frac{x-0.125}{0.125}, if\ 0.125 \le DC\ \le 0.25 \\ \frac{0.325-x}{0.125}, if\ 0.25 \le DC\ \le 0.325 \\ 0, if\ DC > 0.325 \end{Bmatrix} \quad (23)$$

$$d = \begin{Bmatrix} 0, if\ DC < 0.25 \\ \frac{x-0.25}{0.125}, if\ 0.25 \le DC\ \le 0.325 \\ \frac{0.5-x}{0.125}, if\ 0.325 \le DC\ \le 0.5 \\ 0, if\ DC > 0.5 \end{Bmatrix} \quad (24)$$

$$e = \begin{Bmatrix} 0, if\ DC < 0.325 \\ \frac{x-0.325}{0.125}, if\ 0.325 \le DC\ \le 0.5 \\ \frac{0.625-x}{0.125}, if\ 0.5 \le DC\ \le 0.625 \\ 0, if\ DC > 0.625 \end{Bmatrix} \quad (25)$$

$$f = \begin{Bmatrix} 0, if\ DC < 0.5 \\ \frac{x-0.5}{0.125}, if\ 0.5 \le DC\ \le 0.625 \\ \frac{0.75-x}{0.125}, if\ 0.625 \le DC\ \le 0.75 \\ 0, if\ DC > 0.75 \end{Bmatrix} \quad (26)$$

$$g = \begin{Bmatrix} 0, if\ DC < 0.625 \\ \frac{x-0.625}{0.125}, if\ 0.625 \le DC\ \le 0.75 \\ \frac{0.75-x}{0.125}, if\ 0.75 \le DC\ \le 0.875 \\ 0, if\ DC > 0.875 \end{Bmatrix} \quad (27)$$

$$h = \begin{Bmatrix} 0, if\ DC < 0.75 \\ \frac{x-0.75}{0.125}, if\ 0.75 \le DC\ \le 0.875 \\ \frac{1-x}{0.125}, if\ 0.875 \le DC\ \le 1 \\ 0, if\ DC > 1 \end{Bmatrix} \quad (28)$$

$$i = \begin{Bmatrix} 0, if\ DC < 0.875 \\ \frac{x-1}{0.125}, if\ 0.875 \le DC\ \le 1 \\ 1, if\ DC > 1 \end{Bmatrix} \quad (29)$$

The duty cycle response from the fuzzy engine is shown in Fig 3.

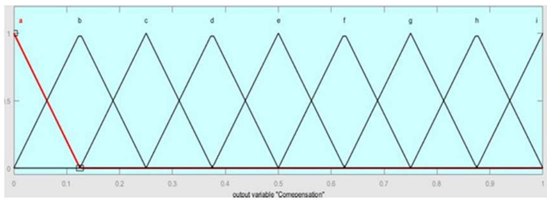

Fig 3. Membership functions for output duty cycle

The input and output membership functions are mapped to one another in the fuzzy controller so that any fluctuation in the rotor speed is measured as a corresponding frequency deviation. The measured deviation is compensated by increasing or decreasing the duty cycle so that the frequency stays near nominal value and within the threshold. The nature of control is also defined to be quick and accelerating for larger deviation and with smaller steps near to the nominal value compassing several sampling instances such that the control action may not introduce abrupt and unnecessary oscillations closer to the required value of frequency. The mapping of input and output is done with the use of linguistic variables commonly called as fuzzy rules in literature. The fuzzy rules for this implementation are listed below:

1. i (29) compensates f if f is equal to -E (12).

2. h (28) compensates f if f is equal to -L (13).
3. g (27) compensates f if f is equal to -M (14).
4. f (26) compensates f if f is equal to -S (15).
5. e (25) compensates f if f is equal to N (16).
6. d (24) compensates f if f is equal to +S (17).
7. c (23) compensates f if f is equal to +M (18).
8. b (22) compensates f if f is equal to +L (19).
9. a (21) compensates f if f is equal to +E (20).

The plateau of the input-output characteristics of the FIS indicate to the insensitivity region and spreads in the region from 48Hz to 52Hz to minimize the high-frequency oscillation that may be caused by control action of the controller nearer to the control point of 50Hz. This region is the threshold for the steady-state to be free of high-frequency components which can cause poor quality of power for a power system. Either side of the plateau is very sensitive to the change in load and contributes to fast convergence to a steady-state. The input-output characteristic of the FIS system is shown in Fig 4.

The crisp output required for the PWM generator to control the armature voltage by means of the duty cycle is evaluated by the defuzzification method of the center of gravity method (COG). Any frequency input activates at most, two input membership set of Fig. 2. which are mapped to corresponding output membership functions with linguistic variables.

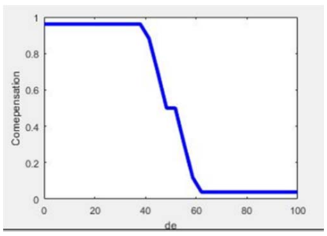

Fig 4. Input-Output Characteristics of FIS

The activated output membership functions compose an area whose center of gravity is calculated. The X coordinated of the center of gravity of hence formed surface corresponds to the crisp duty cycle input required by the PWM converter and is given by (30).

$$Xc = \frac{\sum_{i=0}^{n} XiAi}{\sum_{i=0}^{n} Ai} \qquad (30)$$

Where, n: number of activated sets. X_i: calculated surface center of gravity and A_i: surface area.

III. Simulation Results

The graph shown in Fig 5 demonstrates the simulation result in which the power system is subjected to random load changes equivalent to moderate to severe disturbance.:

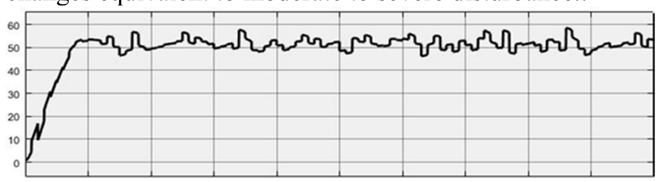

Fig. 5. Output frequency variation of a governor system for high load variation.

The output of the power system is close to nominal value but experiences transients outside of threshold in severe cases. The non-linear signal indicates that the response is rich with harmonic components of both low and high frequency. The Frequency Domain Analysis will be inconclusive as well as inappropriate here as the noise or disturbance is randomized and are non-stochastic as well. The mean of output is 50.08Hz and the median is 51.44Hz; well below tolerance limits. This is indicative of the fact that the control approach is effective and adequate. The following graph is a comparative inspection of the frequency of the power system in the same scenario of moderate to severe disturbance and the corresponding action of the controller. Fig 7 shows the frequency response with the random noise parameter.

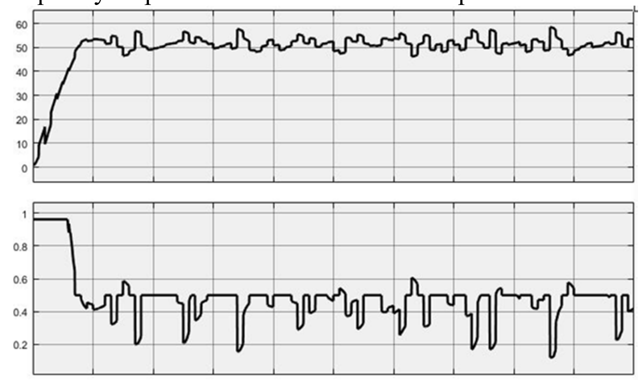

Fig 6. Compensator Output compared to a frequency deviation.

The output of the controller is observed to be quick and without the charging/discharging lags which are common in the PID controller designed or modeled with reactive components and their non-linear response. It can be asserted from the inspection of the graph the FIS response is adequately quick to maintain the mean or median of the frequency of the power system within the threshold boundaries. It should be noted that the disturbances are highly exaggerated in comparison to those experienced by the real power system. The following graph shows the compensated and unloaded power system at the start. The steady-state errors are withing margin and the system reaches the steady-state in time less than one second. The response is critically damped and non-oscillatory which is indicative of the good quality of power generation.

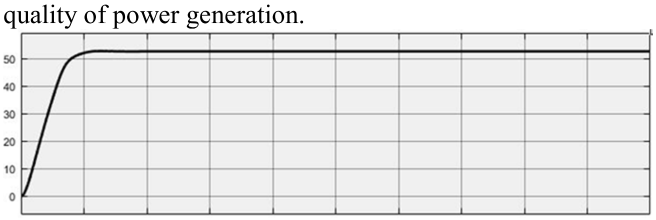

Fig. 7. Frequency Output Response with random noise parameter.

The compensatory response of FIS in the unloaded start of the power system scenario is shown in Fig. 8.

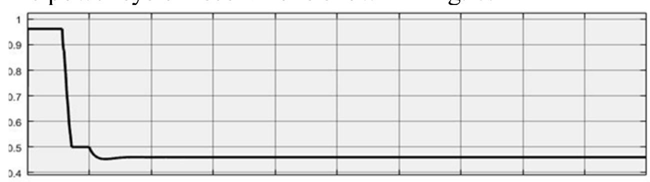

Fig. 8. Compensator response of FIS

Initially, the fuzzy logic controller accelerates the controller output to aid in fast convergence to the nominal value but closer to the nominal value starting from 40Hz mark the response is with decreasing slope and which gets even

978-1-7281-5846-4/20/$31.00 ©2020 IEEE

flattened as the frequency reaches the 48Hz mark. We can observe that the controller is mimicking the control action of a human operator by turning the dial quickly with large steps for a large difference from the nominal value at the start and smaller careful perturbation closer to the nominal value with insensitivity for very small differences.

IV. Hardware Implementation

The FPGA board used in the project is the Xilinx Zybo 7010. Zybo 7010 contains an FPGA based on Zynq architecture. The fuzzy logic controller was implemented in Verilog HDL. The top module contains the instantiations of four submodules: digitization, fuzzification, inference engine, defuzzification. The FPGA receives the input from the sensor in the form of a BCD value, and the digitization module converts the BCD value to decimal and passes it to the fuzzification module. The fuzzification module then fuzzifies the input value and then the inference engine infers a fuzzy output, in which the defuzzification module converts into a crisp value. The top architecture of the Verilog implementation of the fuzzy controller is shown in Fig 9.

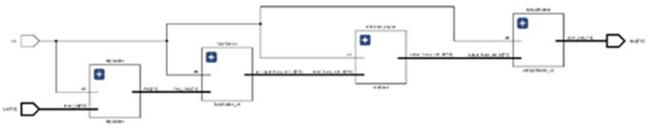

Fig. 9. The top architecture of the Verilog implemented fuzzy logic controller

Table 1 shows the post-implementation resource utilization report for the FPGA.

TABLE 1: POST IMPLEMENTATION RESOURCE UTILIZATION

Resources	Utilization	Available	Utilization Percentage
Look-Up-Tables	130	17600	0.74
Flip-Flops	48	35200	0.14
Input/Output	17	100	17.00

The clock frequency of 125MHz is adequately large from stready state systm frequency of 50Hz. The IR based speedometer is coupled to the shaft of the SG which feeds measured speed to the microcomputer wherein it is translated to corresponding frequency and equations: (12) through (20) are the corresponding numerical interpretation for mapping sensor's reading of speed to the duty cycle. Equations (12) through (20) fuzzify the input frequency and map them to duty cycle membership functions: Equations (21) to (29) which defuzzify the output and translated it to a crisp output of duty cycle percentage for PWM generator controlling armature voltage of DC motor. The COG of the generated area is evaluated and the x-coordinate of the COG which is the required duty cycle for the PWM controller is evaluated with equation (30).

The digital to analog converter supplies the crisp value from the FPGA to the power electronics regulator. The power electronics circuit for controlling the regulation of the voltage to the system is shown in Fig. 10.

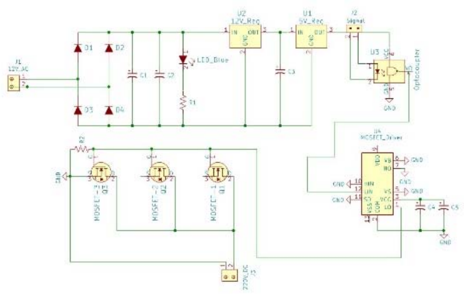

Fig. 10. MOSFET firing circuit

As shown in Fig 10, the diode bridge is used to convert AC to DC to power up the optocoupler MCT and the MOSFET driver IR2110 IC. Three IR830 N-channel MOSFETs are connected in parallel to divide the current, which allows for increased reliability of the circuit. The complete setup of the system is shown in Fig 11.

Fig. 11. FPGA based fuzzy logic controller for synchronous generator

The duty cycle range corresponding to different frequency ranges as measured out of the system are tabulated in Table 2 and the of plot input-output characteristics of the FIS as obtained from the experiments is given in Fig 12.

V. Conclusions

The mathematical model of fuzzy controller is simulated using MATLAB/Simulink environment, and the input-output response of the modeled controller is observed. The simulated controller is then implemented in an FPGA. The setup for testing the hardware-implemented fuzzy controller is constructed in the laboratory, where a separately excited DC motor is used as a prime mover for the alternator. By sampling the shaft speed of the alternator using a tachometer, the frequency of the alternator is calculated, which is then used to infer the output pulse width modulated duty cycle. The PWM technique regulates the voltage supplied to the armature of the DC motor,and controls its speed by varying input voltage. The fuzzy controller generated PWM duty cycle is fed into the gate of the IRF830 MOSFET for voltage regulation. The frequency, duty cycle and voltage output of the system are observed and reported.

It is observed that the response time of the implemented fuzzy controller is instantaneous and precise.. Based on the data obtained, it can be argued that fuzzy controllers are advantageous over conventional controllers whenever the system under control experiences non-linear, unbounded and stochastic disturbances.

978-1-7281-5846-4/20/$31.00 ©2020 IEEE

TABLE 2: DUTY CYCLE AND FREQUENCY CORRESPONDANCE

S No.	Input-Output Relationship		
	Frequency Range	***Duty Cycle Range (%)***	***Output Voltage Range***
01	0 to 40 Hz	96	212 V
02	40 to 42 Hz	95 to 89	210V to 195V
03	42 to 44 Hz	86 to 76	190V to 167V
04	44 to 46 Hz	74 to 64	158V to 140V
05	46 to 48 Hz	61 to 51	134V to 112V
06	48 to 52 Hz	50	110V
07	52 to 54 Hz	49 to 39	108V to 86V
08	54 to 56 Hz	36 to 26	80V to 58V
09	56 to 58 Hz	24 to 14	53V to 30V
11	58 to 60 Hz	12 to 5	26V to 11V
12	60 to 100 Hz	4	9V

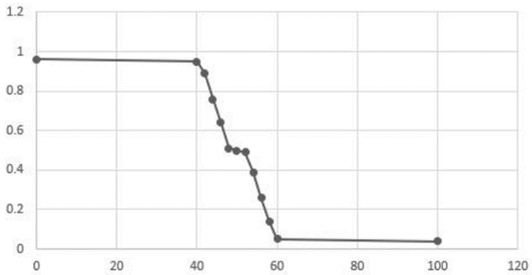

Fig 12. Experimental Input-Output Characteristics of FIS

The execution time of the fuzzy control algorithm heavily depends on the computation time required for each mathematical equation. The sequential execution cycle of traditional microcontrollers demand higher processing speed for the equations but the use of high-speed parallel processing used in our system circumvents this issue by performing concurrent computation of all the equations, thus, minimizing signal propagation delay. The output voltage for the discrete frequency ranges in table I was found to be stable and reliable for slow as well as abrupt disturbances which indicate that the performance of the developed system is adequate for the real power system.

REFERENCES

[1] T. Lahdhiri and A. Alouani, "Non-linear excitation control of a synchronous generator using robust feedback linearization", Optimal Control Applications and Methods, vol. 18, no. 4, pp. 237-256, 1997.

[2] R. Vedam and M. Sarma, Power quality. Boca Raton: CRC Press, 2009.

[3] J. Machowski, J. Bialek, and J. Bumby, Power System Dynamics: Stability and Control, 2nd Edition. John Wiley & Sons, 2008.

[4] P. Subbaraj and K. Manickavasagam, "Automatic generation control of multi-area power system using fuzzy logic controller", European Transactions on Electrical Power, vol. 18, no. 3, pp. 266-280, 2008.

[5] T. Weigert, J. Tsai, and X. Liu, "Fuzzy operator logic and fuzzy resolution", Journal of Automated Reasoning, vol. 10, no. 1, pp. 59-78, 1993.

[6] I. Tamrakar, L. Shilpakar, B. Fernandes and R. Nilsen, "Voltage and frequency control of parallel operated synchronous generator and induction generator with STATCOM in micro-hydro scheme", IET Generation, Transmission & Distribution, vol. 1, no. 5, p. 743, 2007.

[7] S. Laudahn, J. Seidel, B. Engel, T. Bulo and D. Premm, "Substitution of synchronous generator based instantaneous frequency control utilizing inverter-coupled DER", 2016 IEEE 7th International Symposium on Power Electronics for Distributed Generation Systems (PEDG), 2016.

[8] Y. Hsu and W. Chan, "Coordinated Frequency and Voltage Control of Synchronous Generators", IEEE Transactions on Aerospace and Electronic Systems, vol. -23, no. 1, pp. 2-10, 1987.

[9] P. Frack, M. Martinez, M. Molina, and P. Mercado, "Emulation of Synchronous Generator for Frequency Control of Smart Microgrids", IEEE Latin America Transactions, vol. 11, no. 1, pp. 486-491, 2013.

[10] A. Fathi, Q. Shafiee and H. Bevrani, "Robust Frequency Control of Microgrids Using an Extended Virtual Synchronous Generator", IEEE Transactions on Power Systems, vol. 33, no. 6, pp. 6289-6297, 2018.

[11] Y. Wei, I. Jayawardene, Laboratory and G. Venayagamoorthy, "Frequency Prediction of Synchronous Generators in a Multi-Machine Power System with a Photovoltaic Plant Using a Cellular Computational Network", 2015 IEEE Symposium Series on Computational Intelligence, 2015.

[12] A. Pang and P. Membrey, Beginning FPGA: Programming Metal. Apress Media LLC, 2017, p. 3.

[13] S. Hauck and A. DeHon, Reconfigurable Computing: The Theory and Practice of FPGA-based Computation (Morgan Kaufmann series in systems on silicon). Morgan Kaufmann Publishers, 2008, pp. 1-27.

[14] J. Deschamps, G. Bioul and G. Sutter, Synthesis of arithmetic circuits. New York, NY: Wiley-Interscience, 2006, pp. 1-14.

[15] R. Woods, J. McAllister, G. Lightbody, and Y. Yi, FPGA-based implementation of signal processing systems. Chichester: John Wiley & Sons, 2008, pp. 57-76.

[16] U. Meyer-Baese, Digital Signal Processing with Field Programmable Gate Arrays. [New York]: Springer-Verlag Berlin Heidelberg, 2007, pp. 1-25

978-1-7281-5846-4/20/$31.00 ©2020 IEEE